Suprathermal electron production at shock-ignition-relevant conditions characterized by combined methods of x-ray imaging and spectroscopy

O. Renner[1], M. Šmíd[1,2], L. Antonelli[3], D. Batani[3]

[1] *ASCR, Institute of Physics, Prague, Czech Republic*

[2] *Czech Technical University in Prague, FNSPE, Prague, Czech Republic*

[3] *University of Bordeaux, CNRS, CEA, CELIA, UMR 5107, Talence, France*

Generation of suprathermal electrons accompanying interaction of high-intensity lasers with the near-solid density matter represent one of the key issues for realization of alternate schemes of inertial confinement fusion [1]. In the shock ignition approach, a role of hot electrons (hereafter HE) is ambiguous: they contribute to enhancement of the ablation pressure but they may also preheat the pre-compressed targets. A survey of previous HE studies can be found, e.g., in paper [2]. The principal experimental information was collected via x-ray diagnostics. Non-Maxwellian electrons strongly affect properties of x-ray emitting plasma systems, the collisional processes result in creation of holes in inner electronic shells of target atoms and their subsequent filling via radiative transitions. In particular, the $2p \rightarrow 1s$ K-shell fluorescence from a relatively cold target material (usually referred to as Kα emission) studied by advanced x-ray methods provides a direct experimental technique for HE investigation.

We report a novel approach to HE diagnosis based on a combination of monochromatic x-ray imaging and high-resolution K-shell spectroscopy. This research belongs to a series of experiments being performed at PALS laser facility [3] where laser-plasma coupling is studied at intensities up to 5×10^{16} W/cm^2, i.e., at parameters of the laser spike envisaged to launch the shock wave igniting the fusion reaction. We describe the experiment and present recorded x-ray images and K-shell spectra. Benefiting from a detailed ray-tracing analysis of high-resolution methods used, the measured data are interpreted in terms of HE generation. Implications of this procedure for routine diagnosis of suprathermal electrons are briefly discussed.

The experiment was carried out using the fundamental (1ω) and frequency tripled (3ω) radiation of the iodine laser (wavelength λ = 1315/438 nm, pulse duration 0.3/0.25 ns, energy 440/170 J focused to intensities $I = 9\times10^{15}/2\times10^{16}$ W/cm^2 for 1ω/3ω, respectively) striking massive or thin-foil Cu targets at normal incidence. In several shots, an additional 1ω laser beam (60 J, 1×10^{14} W/cm^2) preceding the main pulse by 1.2 ns was used to create a long-scale pre-plasma simulating the compression phase of shock ignition. The implemented diagnostic complex is described elsewhere [2], here we concentrate on high-resolution x-ray diagnosis.

A typical 2D-resolved image of the Cu Kα emission produced by HE interaction with near-surface copper ions is presented in Fig. 1. This distribution of time-integrated signal was recorded with the magnification M = 1.73 (imposed by dimensions of the interaction chamber) on x-ray film Kodak Industrex AA400, digitized with the scanner providing spatial resolution of 5.3 μm and converted to incident photon fluxes with respect to the characteristic curve of the film and filter transmission. The observed elliptical shape of the emitting area corresponds to an oblique line of sight of the imager observing the target surface at angle of ~45°. The images were recorded with the crystal of quartz (422) spherically bent to a radius of 380 mm. The combination of Cu Kα radiation with the photon energy 8047.8 eV and the crystal interplanar spacing 2d = 0.15414 nm results in the quasi-normal incidence configuration of the imaging system with the central Bragg angle θ_B = 88.15°. Taking into account the source-to-crystal distance of 300 mm and the circular crystal aperture of 24 mm, the range of photon energies reflected from the crystal surface is limited to 3.86 eV which is comparable with the FWHM width of the cold Cu $K\alpha_1$ emission (2.29 eV). The signal collected by the crystal obviously corresponds only to a fraction of the K-shell emission due to HE action. To remedy this, the recorded signal has to be corrected for a limited spectral coverage, i.e., the imaging must be complemented by information obtained via high-resolution spectroscopy.

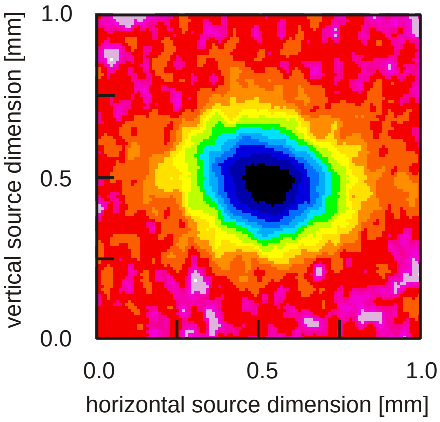

Fig. 1. Distribution of Cu K-shell emission from the 1ω-irradiated 10-μm-thick foil visualized by monochromatic imaging.

The K-shell spectra were observed at an angle of 10° to the target surface by using the x-ray spectrometer equipped with the crystal of quartz (223) spherically bent to a radius of 150 mm. The spectrometer was aligned to cover the photon energy range of 7.9–8.5 keV and provided the 1D spatial resolution of 14 μm in a direction of the target normal. The spectra were again recorded on x-ray film, calibrated with respect to dispersion relation of the experimental geometry used and cross-checked via tabulated dominant Cu K-shell transitions (Kα doublet and the resonance w and intercombination y line of He-like Cu). The signal was recalculated to an intensity scale with respect to a variable crystal reflectivity and transmission through filters.

The spectra shown in Fig. 2 demonstrate clearly the effect of the laser coupling parameter. Whereas at 1ω the laser-matter interaction results in an increased emission of inner shell electronic transitions in less ionized atoms (Kα transitions in single-ionized Cu II atoms

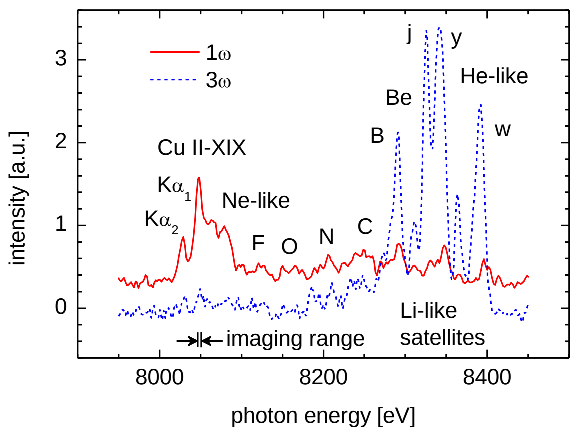

Fig. 2. X-ray spectra emitted from Cu targets subject to 1ω and 3 ω laser radiation.

overlapped by Cu III till Cu XIX emission), the 3ω Cu K-shell emission is governed by the resonance line transitions in highly ionized atoms and their satellites (so-called quasi-optical transitions). Complementary spectral structure observed between Kα and Heα lines belongs to emission from Li- till Ne-like copper ions. The presence of these transitions in emitted x-ray spectra generally indicates an occurrence of suprathermal electrons with the energy above the K-shell ionization limit of the atom in a given ionization state. Detailed quantitative interpretation of these spectral features is complicated due to their dependence on two factors, the HE production as a driving force and the presence of the colder, variable-temperature target material as a diagnostic medium [4]. On the other hand, spectra modelling using the FLYCHK code [5] clearly indicates that the occurrence of Kα to Ne-like transitions refers to the HE action in Cu characterized by the bulk temperature $T \leq 200$ eV whereas optimum conditions for emission of C-like ions under the presence of HE correspond to $T \leq 800$ eV. Consequently, the recorded spectra can be interpreted in terms of the HE evolution and interaction in early phases of the target irradiation or via their transport through lower-T material. The found intensity ratios between the 3.86 eV-wide spectral range covered by the imaging (see Fig. 2) and intensities integrated over the ranges of 8–8.1 keV (characterizing the HE interaction with the colder plasma) or 8–8.265 keV (covering wider range of bulk plasma temperatures) were used for rigorous evaluation of K-shell fluorescence which is of primary importance for interpretation of 2D images.

The interpretation of K-shell images in terms of the HE generation proceeded in three steps. First the Cu Kα signal recorded above the detector background was recalculated to the source emission, then this intermediate product was corrected with respect to the limited spectral range of the imaging and finally the resulting full K-shell emission was related to the number of suprathermal electron propagating through the Cu target.

The first problem was solved via application of a detailed quantitative ray-tracing analysis [6]. The computed transfer characteristics of the imaging system relate one photon recorded at detector to 5.2×10^5 monochromatic photons emitted from the source to 4π. For spectrometer, the required number of emitted photons increases to 4.4×10^7. The validity of calculations was proved by comparing the photon fluxes measured close to Cu Kα maximum in the spectral window ΔE_i=3.86 eV defined by the imaging; the emitted intensities found for individual shots spanned the range of 1–6×10^{10} photons/4π and were identic for imaging and spectroscopy within the error bars (~40%). The full number of K-shell photons emitted into the energy ranges of ΔE=100 or 265 eV was determined from imaging records by multiplying their integrated signals with a factor relating spectral intensities measured within the above defined ranges of ΔE and ΔE_i. The found photon fluxes were related to the number of generated HE using previously described procedure [7], HE characteristic temperatures of 50 keV (measured for 1ω) and 26 keV (derived from Beg's scaling law [8] for 3ω) and thin target approximation.

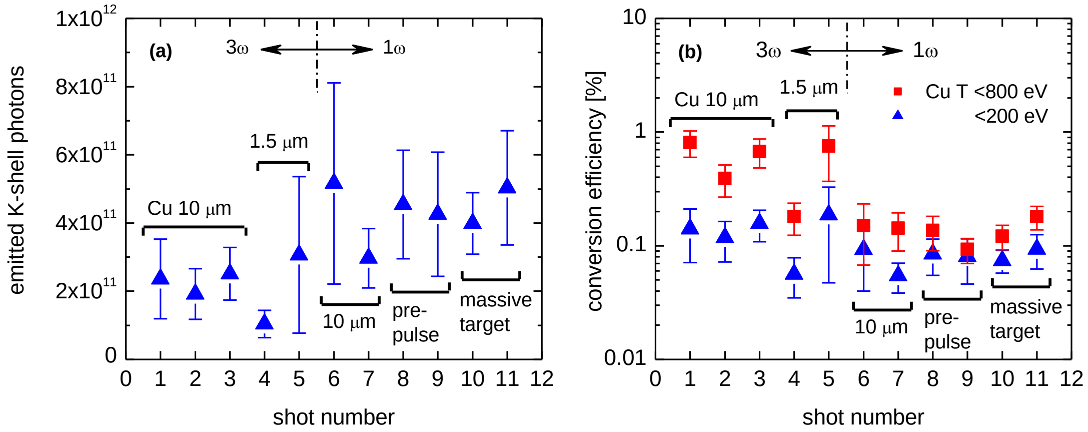

Fig. 3. Photon fluxes reconstructed from x-ray images for ΔE=100 eV (a) and laser energy conversion efficiency into hot electrons (b). Diverse Cu targets were irradiated by 1ω and 3ω laser beams focused to diameter 100 μm.

An example of found characteristics is presented in Fig. 3. The emitted photon fluxes derived from the imaging and corrected via spectroscopic data are related to conversion efficiency of suprathermal electron generation at diverse conditions of target irradiation. The interpretation of the experimentally obtained results proceeds and will be published elsewhere.

To conclude, K-shell imaging combined with high resolution x-ray spectroscopy offers a novel method for hot electron diagnosis. Despite simplifications currently used in evaluation of experimental data, the obtained results demonstrate viability of this method for characterization of suprathermal electrons in shock-ignition-relevant plasmas.

This work benefitted from the support of the Czech Science Foundation project CZ.1.07/2.3.00/20.0279 and the Academy of Sciences Programme for internal support of international collaboration, project M100101208.

References

[1] S.Yu. Guskov, Plasma Phys. Reports **39** (2013) 12013.
[2] P. Köster et al, Plasma Phys. Control. Fusion **55** (2013) 124045.
[3] K. Jungwirth et al, Phys. Plasmas **8** (2001) 2495.
[4] M. Šmíd et al, Phys. Scr. **T145** (2014) 014020.
[5] H.K. Chung et al, High Energy Density Phys. **1** (2005) 3.
[6] S.G. Podorov et al, J. Phys. D: Appl. Phys. **34** (2001) 2363.
[7] A. Morace and D. Batani, Nucl. Instr. Meth. Phys. Res. **A623** (2010) 797.
[8] F.N. Beg et al, Phys. Plasmas **4** (1997) 447.